Pacific Northwest
NATIONAL LABORATORY

PNNL-37623 Rev 0
DFTP-RPT-048 Rev 0

Strontium Speciation in Relevant Tank Waste Components Examined by Electrospray Ionization Mass Spectrometry

July 2025

Amanda R. Bubas
Elise R. Conte
Richard M Cox
Tatiana G. Levitskaia
Emily L. Campbell
Reid A. Peterson

U.S. DEPARTMENT of ENERGY

Prepared for the U.S. Department of Energy
under Contract DE-AC05-76RL01830

DISCLAIMER

PACIFIC NORTHWEST NATIONAL LABORATORY
operated by
BATTELLE
for the
UNITED STATES DEPARTMENT OF ENERGY
under Contract DE-AC05-76RL01830

Printed in the United States of America

Available to DOE and DOE contractors from
the Office of Scientific and Technical Information,
P.O. Box 62, Oak Ridge, TN 37831-0062
www.osti.gov
ph: (865) 576-8401
fox: (865) 576-5728
email: reports@osti.gov

Available to the public from the National Technical Information Service
5301 Shawnee Rd., Alexandria, VA 22312
ph: (800) 553-NTIS (6847)
or (703) 605-6000
email: info@ntis.gov
Online ordering: http://www.ntis.gov

PNNL-37623 Rev 0
DFTP-RPT-048 Rev 0

Strontium Speciation in Relevant Tank Waste Components Examined by Electrospray Ionization Mass Spectrometry

July 2025

Amanda R. Bubas
Elise R. Conte
Richard M Cox
Tatiana G. Levitskaia
Emily L. Campbell
Reid A. Peterson

Prepared for
the U.S. Department of Energy
under Contract DE-AC05-76RL01830

Pacific Northwest National Laboratory
Richland, Washington 99354

Abstract

The identification of chemical species formed in complex nuclear waste is crucial for the development and employment of advanced separations technologies to remediate the Hanford site by processing tank waste. The current Tank Side Cesium Removal (TSCR) process deployed at Hanford utilizes crystalline silicotitanate (CST) ion exchange (IX) media to aid in the separation of low-activity waste for proper treatment and disposal. The inorganic IX media is highly selective for Cs but has been shown to also remove Sr from caustic simulants and small-scale IX processing of Hanford tank waste.(Fiskum, Rovira et al. 2019, Fiskum, Campbell et al. 2021, Westesen, Campbell et al. 2022) Quantitative Sr removal has not been observed in all tank waste supernates tested; thus, to better understand Sr removal and effectively predict processing behavior through TSCR, it is necessary to first investigate Sr speciation in tank waste. This work utilized electrospray ionization mass spectrometry (ESI-MS) to identify ionic Sr complexes that form in the presence of NO_3^-, NO_2^-, OH^-, and Cl^-. Although our results show that NO_3^-, NO_2^-, and OH^- are competitive for Sr^{2+} binding, previous data from IX studies indicate that $[SrOH]^+$ is not the dominant species of concern in tank waste processing schemes.(Fiskum, Campbell and Trang-Le 2020) Our results show that the $[Sr(NO_3)]^+$ species and the $[Sr(NO_2)]^+$ species form in considerable abundances, which may affect the ability to separate Sr using CST in nuclear waste separation processes.

Summary

The primary objective of the present study is to utilize electrospray ionization mass spectrometry (ESI-MS) to better understand the complexation chemistry of Sr in Hanford tank waste. A better understanding of the speciation of Sr in tank waste media is necessary to predict the transport and fate of Sr in nuclear waste processing systems. Hanford tank waste contains a mixture of complexing agents, including NO_3^-, NO_2^-, OH^-, and Cl^- that form soluble Sr salts and are of particular interest for the present investigation. The competition between these complexing anions in nuclear waste for Sr binding is also assessed by comparing the relative abundances of the observed ionic species. The present ESI-MS results show that Sr^{2+} binds with NO_3^-, NO_2^-, OH^- and to a lesser extent Cl^-. Ion exchange studies have concluded that $[SrOH]^+$ is not the dominant Sr species of concern in the tank side cesium removal process.(Fiskum, Campbell and Trang-Le 2020) $[Sr(NO_3)]^+$ and $[Sr(NO_2)]^+$ were observed in comparable abundances to $[SrOH]^+$ and may influence the ability to separate Sr in tank waste processing schemes.

Acknowledgments

This work was supported by H2C (formally known as Washington River Protection Solutions). Pacific Northwest National Laboratory (PNNL) is a multiprogram national laboratory operated for the U.S. Department of Energy by Battelle Memorial Institute under Contract No. DE-AC05-76RL01830.

Acronyms and Abbreviations

TSCR	Tank Side Cesium Removal
CST	Crystalline Silicotitanate
IX	Ion Exchange
ESI-MS	Electrospray Ionization Mass Spectrometry
ICP-MS	Inductively Coupled Plasma Mass Spectrometry
IRMPD	Infrared Multiple-Photon Dissociation
MeOH	Methanol
EtOH	Ethanol
CID	Collision-Induced Dissociation
TSQ	Triple Stage Quadrupole
WARM	West Area Risk Management

Contents

Abstract ii
Summary iii
Acknowledgments iv
Acronyms and Abbreviations v
1.0 Introduction 1
2.0 Methods 4
2.1 Sample Preparation 4
2.2 Sample Analysis by ESI-MS and ESI-MS/MS 5
3.0 Results 6
3.1 Strontium Nitrate Complexation 6
3.2 Competition of Nitrate and Nitrite for Sr 8
3.3 Competition of Nitrate and Hydroxide for Sr 14
3.4 Competition of Nitrate and Chloride for Sr 16
3.5 Competition of Nitrate, Nitrite, Hydroxide, and Chloride for Sr 20
4.0 Relevance to Hanford Tank Waste Separations 24
5.0 Conclusion 26
6.0 Ongoing Work and Future Directions 27
6.1 Part of West Area Risk Management (WARM) Project 27
6.2 ESI-MS Experiments 27
6.2.1 Competition Assessments 27
6.2.2 Effect of pH upon the Observed Mass Spectrum 27
6.2.3 Quantitative Analysis 28
6.3 Analysis by Inductively Coupled Plasma Mass Spectrometry 28
7.0 References 29

Figures

Figure 1. Positive ESI-MS and ESI-MS/MS spectra of $Sr(NO_3)_2$ in 50:50 (by volume) MeOH:H_2O (left) and 50:50 (by volume) EtOH:H_2O (right).....

Figure 2. (Top to bottom) Negative a) ESI-MS of $Sr(NO_3)_2$ in MeOH and H_2O and ESI-MS/MS spectra of b) $[Sr_2(NO_3)_5]^-$ (486 m/z), c) $[Sr(NO_3)_3]^-$ (274 m/z), and d) $[NO_3]^-$ (62 m/z). .....

Figure 3. (Top to Bottom) a) Positive ESI-MS of $Sr(NO_3)_2$ in MeOH and H_2O and ESI-MS/MS spectra of b) $[Sr_2(NO_3)_3]^+$ (362 m/z), c) $[Sr(NO_3)]^+$ (150 m/z), d) $[Sr(O_2)]^+$ (120 m/z), and e) $[Sr(O)]^+$ (104 m/z). .....

Figure 4. Negative (top) and positive (bottom) ESI-MS (20-500 m/z) of ~1:2 $Sr(NO_3)_2$:$NaNO_2$ in MeOH and H_2O. .....

Figure 5. (Top to bottom) Negative a) ESI-MS of ~1:2 $Sr(NO_3)_2$:$NaNO_2$ in MeOH and H_2O and ESI-MS/MS spectra of b) $[Sr_2(NO_2)_2(NO_3)_3]^-$ (454 m/z), c) $[Sr_2(NO_2)_3(NO_3)_2]^-$ (438 m/z), d) $[Sr_2(NO_2)_4(NO_3)]^-$ (422 m/z), e) $[Sr(NO_2)(NO_3)_2]^-$ (258 m/z), f) $[Sr(NO_2)_2(NO_3)]^-$ (242 m/z), and g) $[Sr(NO_2)_3]^-$ (226 m/z). .....

Figure 6. (Top to bottom) Positive a) ESI-MS of ~1:2 $Sr(NO_3)_2$:$NaNO_2$ in MeOH and H_2O and ESI-MS/MS spectra of b) $[Sr_2(NO_2)(NO_3)_2]^+$ (346 m/z), c) $[Sr_2(NO_2)_2(NO_3)]^+$ (330 m/z), d) $[Sr_2(NO_2)_3]^+$ (314 m/z), and e) $[Sr(NO_2)]^+$ (134 m/z). .....

Figure 7. Negative (top) and positive (bottom) ESI-MS (10-500 m/z) of ~1:2 $Sr(NO_3)_2$:NH_4OH in MeOH and H_2O (black traces) are superimposed upon the respective negative and positive ESI-MS spectra for $Sr(NO_3)_2$ (blue traces) in MeOH and H_2O.....

Figure 8. Negative (top) and positive (bottom) ESI-MS (10-500 m/z) of ~1:2 $Sr(NO_3)_2$:NaOH in MeOH and H_2O (black traces) are superimposed upon the respective negative and positive ESI-MS spectra for $Sr(NO_3)_2$ (blue traces) in MeOH and H_2O.....

Figure 9. Negative (top) and positive (bottom) ESI-MS spectra (20-500 m/z) of ~1:1 $Sr(NO_3)_2$:$SrCl_2$ in MeOH and H_2O. Inset spectra are included to show ions containing Sr complexed to a mixture of nitrate and chloride ligands more clearly. .....

Figure 10. (Top to bottom) Negative a) ESI-MS spectrum (20-500 m/z) of ~1:1 $Sr(NO_3)_2$:$SrCl_2$ in MeOH and H_2O and ESI-MS/MS spectra of b) $[Sr_2{}^{35}Cl(NO_3)_4]^-$ (459 m/z), c) $[Sr_2{}^{35}Cl_2(NO_3)_3]^-$ (432 m/z), d) $[Sr_2{}^{35}Cl_3(NO_3)_2]^-$ (405 m/z), e) $Sr_2{}^{35}Cl_4(NO_3)]^-$ (378 m/z), f) $[Sr^{35}Cl(NO_3)_2]^-$ (247 m/z), and g) $[Sr^{35}Cl_2(NO_3)]^-$ (220 m/z). .....

Figure 11. (Top to bottom) Positive a) ESI-MS spectrum (20-500 m/z) of ~1:1 $Sr(NO_3)_2$:$SrCl_2$ in MeOH and H_2O and ESI-MS/MS spectra of b) $[Sr_2{}^{35}Cl(NO_3)_2]^+$ (335 m/z), and c) $[Sr_2{}^{35}Cl_2(NO_3)]^+$ (308 m/z). .....

Figure 12. Negative (top) and positive (bottom) ESI-MS spectra (20-500 m/z) of ~1:1 $Sr(NO_3)_2$:$SrCl_2$ in MeOH and H_2O superimposed upon the respective negative and positive ESI-MS spectra of the individual $Sr(NO_3)_2$ (blue trace) and $SrCl_2$ (orange trace) ESI solutions. .....

Figure 13. The negative (top) and positive (bottom) ESI-MS spectra for ~1:2:2:1 $Sr(NO_3)_2$:$NaNO_2$:NH_4OH:$SrCl_2$ (so that concentrations of the complexing anions are ~1:1:1:1) in MeOH and H_2O.....

Figure 14. The negative (top) and positive (bottom) ESI-MS spectra for ~1:2:2:1 $Sr(NO_3)_2$:$NaNO_2$:NaOH:$SrCl_2$ (so that concentrations of the complexing anions are ~1:1:1:1) in MeOH and H_2O.....

1.0 Introduction

Environmental management and waste remediation efforts at the Hanford site remain a priority for the United States Department of Energy. Contents of Hanford tank waste include radioactive and chemical waste from nuclear fuel reprocessing and plutonium production for nuclear weapons development dating back to World War II. The resulting nuclear waste has been accumulated over several decades, and consequently, waste streams from several processes used to treat spent fuel have been combined, resulting in increasingly complex mixed waste unique to each tank.(Colburn and Peterson 2021) Proper treatment of the existing waste involves sequestration of high activity components (such as cesium) from low activity waste so that low activity waste can treated and immobilized for on-site storage. High activity components can be blended with long lived isotopes, vitrified, stored in stainless steel canisters, and transported to a designated geological repository.(Peterson, Buck et al. 2018) However, one option currently being explored is shipment of the low activity waste off-site. To enable this option, it may be necessary to remove additional radionuclides from the supernatant waste. It is important to identify the species present in the target waste media to effectively and efficiently employ existing separations technologies. An accurate identification of the species generated in complex tank wastes will also serve to revise and improve existing models used to predict the chemical properties and evolution of tank waste.

Strontium has been identified as a hazardous radionuclide due to its high fission yield (4 – 5%) and high activity with a 28-year half-life. To enable off-site shipment of waste, strontium may also need to be removed in the cesium tank side separation processes. Crystalline silicotitanate (CST) ion exchange media is selective for Cs removal. Tank waste processing schemes employing CST as the ion exchange media revealed significant uptake of the group II metals Ca, Sr, and Ba.(Fiskum, Rovira et al. 2019, Campbell, Westesen et al. 2021, Fiskum, Campbell et al. 2021, Fiskum, Westesen et al. 2021) Initially, this caused some concern that

group II metal complexes may occupy Cs exchange sites, thereby reducing Cs uptake and removal from tank waste. The group II metal hydroxide, MOH^+, was initially suspected to be the interfering species of interest.(Hamm 2004) However, testing demonstrated that these group II metals did not significantly interfere with cesium removal, and further analysis suggested that $[SrOH]^+$ was not the dominant Sr species of concern.(Fiskum, Campbell and Trang-Le 2020)

Information related to the complexation and speciation chemistry of strontium in aqueous nuclear waste streams is limited. Nuclear waste is complex and offers a variety of coordinating ligands including NO_3^-, NO_2^-, OH^-, Cl^-, CO_3^{2-}, SO_4^{2-}, and PO_4^{3-}. In aqueous media, strontium nitrate, nitrite, and chloride salts are generally soluble, and strontium hydroxide is slightly soluble. Strontium carbonate, sulfate, and phosphate salts are comparatively insoluble; therefore, it is anticipated that these complexes precipitate out of solution. This likely limits the ability of carbonate, sulfate, and phosphate complexes to cause extensive issues in aqueous waste stream processing schemes.

Electrospray ionization mass spectrometry (ESI-MS) is advantageous for the identification of complex species present in solution because it is a “soft ionization” technique that can be used to transfer intact ionic species into the gas phase with minimal fragmentation generally preserving the solution phase speciation present (in contrast to ICP-MS where all speciation is obliterated when the sample is completely atomized).(Fenn, Mann et al. 1989, Fenn, Mann et al. 1990) Previous ESI-MS studies and infrared multiple-photon dissociation (IRMPD) spectroscopy experiments have enabled the identification of metal nitrate and metal nitrite species.(Li, Byers and Houk 2003, Oomens, Myers et al. 2008, Leavitt, Oomens et al. 2009, Frański, Sobieszczuk and Gierczyk 2014, Frański 2015, Fraſski, Osiſska and Gierczyk 2016, Bubas, Perez et al. 2021) Van Stipdonk and coworkers reported a tandem mass spectrometry (MS^n) investigation of the uranyl cation coordinated by a mixture of formate and acetate ligands.(Bubas, Tatosian et al. 2024) Collision-induced dissociation (CID) of the

$[UO_2(H)(O_2C\text{-}CH_3)(O_2C\text{-}H)]^-$ precursor revealed preferential elimination of formaldehyde over acetaldehyde. The results of this prior ESI-MS^n study provided the foundation for the present study, specifically that ESI-MS/MS may be a useful method to assess competition between ligands for metal binding. The primary objectives of the present study are to better understand the complexation chemistry of Sr in the presence of mixed nuclear waste components (NO_3^-, NO_2^-, OH^-, and Cl^-) using ESI-MS and assess the competition of these complexing anions in nuclear waste for Sr binding. The present results indicate that OH^-, NO_3^-, and NO_2^- ligands are strong competitors for Sr^{2+} binding, but $[Sr(NO_3)]^+$ and $[Sr(NO_2)]^+$ may influence the ability to separate Sr in tank waste processing schemes utilizing the CST ion exchange media.

2.0 Methods

2.1 Sample Preparation

Separate 5 mL stock solutions (0.2 mM) of $Sr(NO_3)_2$, $NaNO_2$, NH_4OH, NaOH, and $SrCl_2$ were prepared by dissolving the respective salt in deionized H_2O. 20-40 µL of the prepared stock solutions were combined and further diluted in 2000 µL of 50:50 (by volume) MeOH and deionized H_2O and used as the spray solution for ESI-MS and subsequent collision-induced dissociation (CID) experiments. Experiments using the $Sr(NO_3)_2$ solution diluted in 50:50 (by volume) EtOH:H_2O were also conducted so that mass losses of 32 amu and 46 amu could accurately be attributed to either the elimination of O_2 and NO_2 or the elimination of MeOH and EtOH (32 and 46 amu) that otherwise would not be easily distinguished with the limited resolution of the ESI-MS. Fragmentation patterns of the ions generated by ESI of $Sr(NO_3)_2$ in separate MeOH and EtOH solvents are shown in Figure 1.

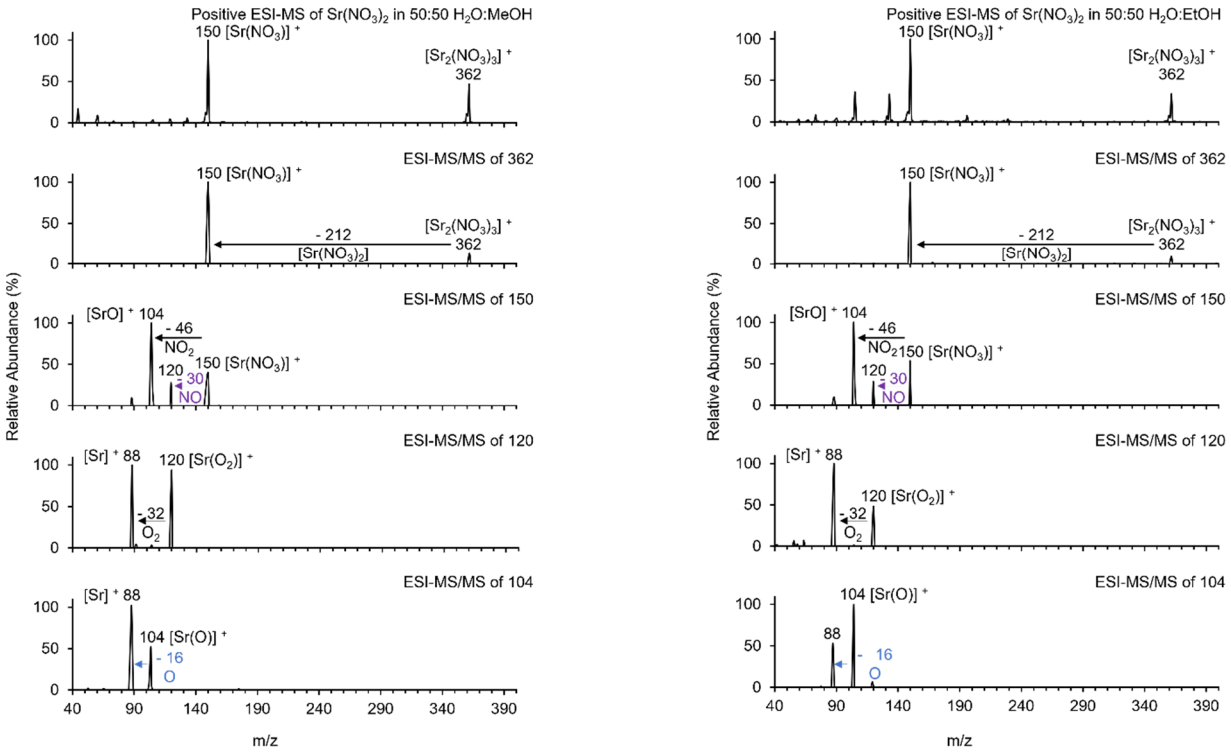

Figure 1. Positive ESI-MS and ESI-MS/MS spectra of $Sr(NO_3)_2$ in 50:50 (by volume) MeOH:H_2O (left) and 50:50 (by volume) EtOH:H_2O (right).

A comparison of the resulting ESI-MS and ESI-MS/MS spectra shows that the observed mass losses are consistent regardless of whether MeOH or EtOH was used as the cosolvent in the ESI spray solutions; therefore, mass losses of 32 and 46 amu are attributed to fragmentation of the NO_3^- ligand leading to losses of O_2 and NO_2.

2.2 Sample Analysis by ESI-MS and ESI-MS/MS

The ESI-MS and CID experiments were conducted using a ThermoScientific Triple Stage Quadrupole (TSQ) Quantum Access Max mass spectrometer. The spray solutions were directly infused into the mass spectrometer using a syringe pump with a flow rate of 5-10 µL /minute. The ionization settings were optimized in both the positive and negative ion modes (spray voltage of +2700 or -3000 V for positive and negative modes, respectively, sheath gas pressure of 15 arbitrary units, and capillary temperature of 250 degrees Celsius). Tube lens offset and skimmer offset voltages were optimized using the auto tune routine with the TSQ software for maximum precursor ion transmission. Nitrogen was used as the desolvation gas, and argon was used as the collision gas for CID experiments.

3.0 Results

ESI-MS enables an examination of species present in solution and provides qualitative and quantitative stoichiometric information that correlates with observations from solution phase chemistry experiments.(Glish and Vachet 2003, Schröder 2012) Nevertheless, a brief discussion of the solution phase conditions that are not necessarily reflected in the ESI-MS spectrum is required for an informed interpretation of the results. Despite the gentle nature of the electrospray ionization process and its ability to preserve chemical complexation, changes in concentration, pH, and solvation are probable.(Kebarle and Verkerk 2009) The choice of a protic (methanol) or aprotic (acetonitrile) solvent will also influence the species observed in the resulting spectrum.(McMahon and Kebarle 1977) Additionally, charged species are preferentially detected, and neutral species may only be detected if they undergo some type of cationization or deprotonation event during the ionization process.(Schröder 2012) Conversely, some detected species may be more easily generated or only exist in the gas phase that are otherwise unstable or unable to form in solution (i.e. because of oxidation states). These considerations are important, though they do not diminish the ability and utility of ESI-MS to predict the chemical species that may form in the solution phase.

3.1 Strontium Nitrate Complexation

A previous study included an examination of the ESI-MS/MS spectrum of $[Sr(NO_3)_3]^-$.(Frański, Sobieszczuk and Gierczyk 2014) Upon collision-induced dissociation, this precursor ion undergoes elimination of neutral $Sr(NO_3)_2$ to leave the bare nitrate anion, $[NO_3]^-$. Our results are shown in Figure 2.

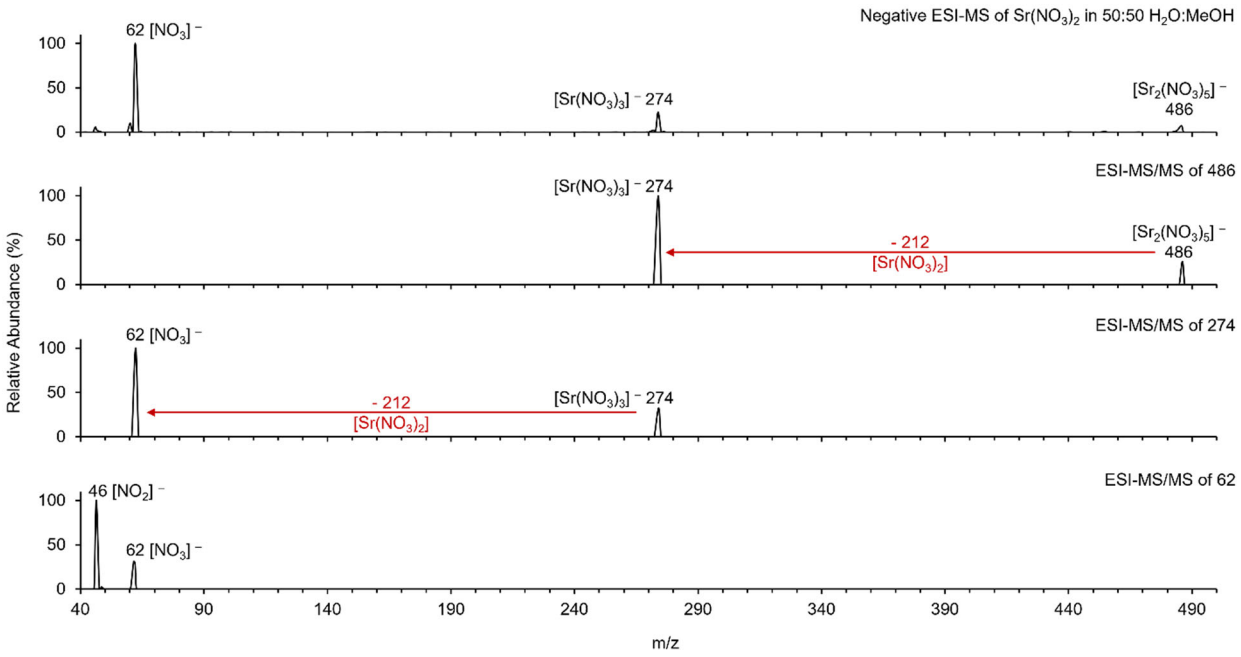

Figure 2. (Top to bottom) Negative a) ESI-MS of $Sr(NO_3)_2$ in MeOH and H_2O and ESI-MS/MS spectra of b) $[Sr_2(NO_3)_5]^-$ (486 m/z), c) $[Sr(NO_3)_3]^-$ (274 m/z), and d) $[NO_3]^-$ (62 m/z).

Over the mass range of 40 – 500 m/z, the $[Sr_2(NO_3)_5]^-$ cluster anion (486 m/z), $[Sr(NO_3)_3]^-$ (274 m/z), and $[NO_3]^-$ (62 m/z) were observed in the ESI-MS spectrum. The ESI-MS/MS spectrum of the $[Sr_2(NO_3)_5]^-$ cluster anion reveals that $[Sr_2(NO_3)_5]^-$ eliminates neutral $Sr(NO_3)_2$ to form $[Sr(NO_3)_3]^-$. Subsequent CID of the $[Sr(NO_3)_3]^-$ precursor leads to the elimination of neutral $Sr(NO_3)_2$ to leave the bare nitrate anion, $[NO_3]^-$, as was observed in the previous study.(Frański, Sobieszczuk and Gierczyk 2014)

The ESI-MS/MS data for cationic strontium nitrate species have also been previously reported.(Frański 2015) Our results are consistent with the previously reported results and are found in Figure 3.

$[Sr_2(NO_3)_3]^+$ (362 m/z) and $[Sr(NO_3)]^+$ (150 m/z) were observed over the 40 – 500 m/z range.

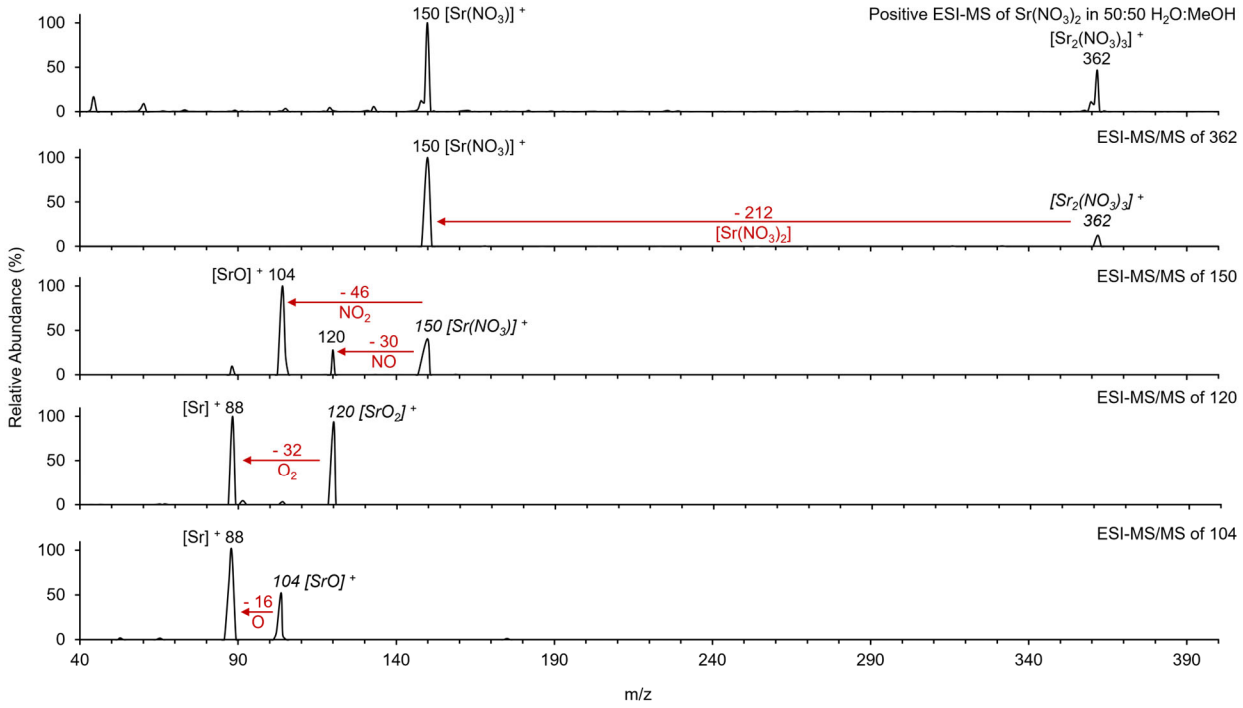

Figure 3. (Top to Bottom) a) Positive ESI-MS of $Sr(NO_3)_2$ in MeOH and H_2O and ESI-MS/MS spectra of b) $[Sr_2(NO_3)_3]^+$ (362 m/z), c) $[Sr(NO_3)]^+$ (150 m/z), d) $[Sr(O_2)]^+$ (120 m/z), and e) $[Sr(O)]^+$ (104 m/z).

Fragmentation of the $[Sr_2(NO_3)_3]^+$ cation cluster leads to the elimination of neutral $Sr(NO_3)_2$ to yield $[Sr(NO_3)]^+$. Subsequent CID of $[Sr(NO_3)]^+$ leads to a loss of NO (30 amu) to form $[SrO_2]^+$ as the minor product ion at 120 m/z, and a loss of NO_2 (46 amu) to form $[SrO]^+$ as the dominant product ion at 104 m/z. Fragmentation of $[SrO_2]^+$ at 120 m/z leads to formation of the bare Sr^+ ion at 88 m/z through the elimination of O_2 (32 amu). Fragmentation of $[SrO]^+$ at 104 m/z also leads to formation of Sr^+.

3.2 Competition of Nitrate and Nitrite for Sr

The negative ESI-MS spectrum (20-500 m/z) of a ~1:2 $Sr(NO_3)_2$:$NaNO_2$ (1:2 by concentration, so that $[NO_3^-]\approx[NO_2^-]$) in 50:50 (by volume) MeOH:H_2O is shown in Figure 4 (top).

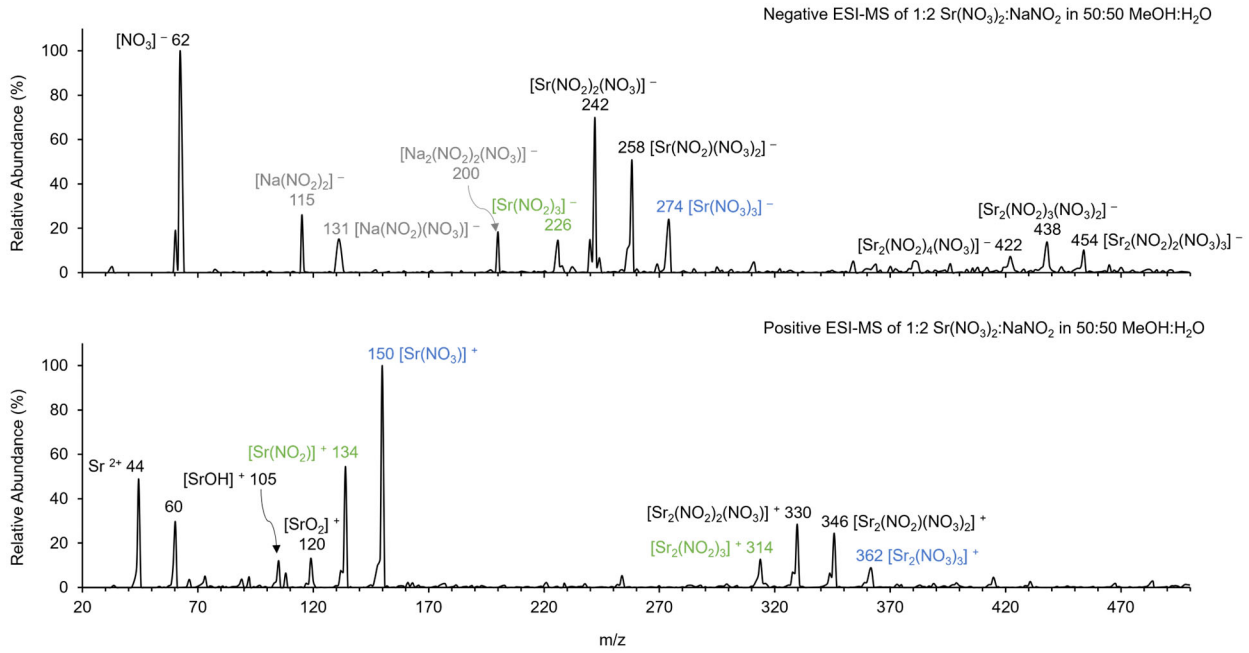

Figure 4. Negative (top) and positive (bottom) ESI-MS (20-500 m/z) of ~1:2 $Sr(NO_3)_2$:$NaNO_2$ in MeOH and H_2O.

The dominant species at 62 m/z is the bare nitrate anion, $[NO_3]^-$. Interestingly, the bare nitrite anion, $[NO_2]^-$, at 46 m/z was not observed, which may indicate that nitrite is complexed as neutral $NaNO_2$ or $Sr(NO_2)_2$, neither of which would be detected by ESI-MS. The $[Sr(NO_3)_3]^-$ product was observed at 274 m/z, $[Sr(NO_2)(NO_3)_2]^-$ at 258 m/z, $[Sr(NO_2)_2(NO_3)]^-$ at 242 m/z, and $[Sr(NO_2)_3]^-$ at 226 m/z. $[Sr(NO_2)_2(NO_3)]^-$ at 242 m/z is the most abundant Sr-containing species observed, followed by $[Sr(NO_2)(NO_3)_2]^-$ at 258 m/z, demonstrating competition between nitrate and nitrite for Sr binding. The relative abundances of the $[Sr(NO_3)_3]^-$ and $[Sr(NO_2)_3]^-$ species suggest that NO_3^- may be slightly more competitive for Sr than NO_2^-. Alternatively, formation of the neutral $Sr(NO_2)_2$ species may be a dominant process that cannot be directly determined by ESI-MS but would result in reduced intensities observed for ionic strontium nitrite containing species as well as the bare nitrite anion. Anionic strontium cluster complexes incorporating a mixture of nitrate and nitrite ligands were also observed at 454 m/z, 438 m/z, and 422 m/z, corresponding to $[Sr_2(NO_2)_2(NO_3)_3]^-$, $[Sr_2(NO_2)_3(NO_3)_2]^-$, and $[Sr_2(NO_2)_4(NO_3)]^-$,

respectively. ESI-MS/MS spectra detailing the CID of the ions at 454, 438, 422, 258, 242, and 226 m/z can be found in Figure 5.

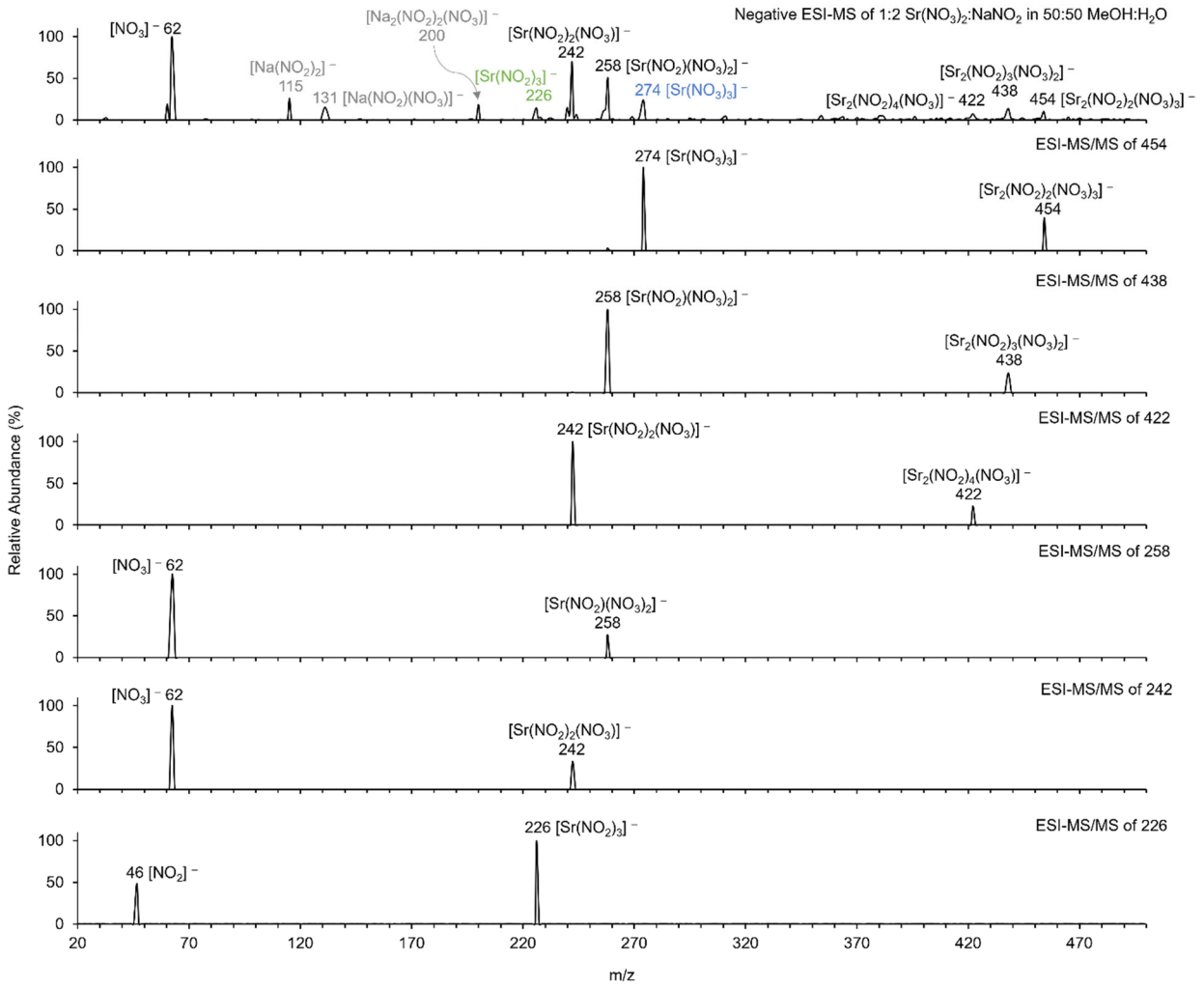

Figure 5. (Top to bottom) Negative a) ESI-MS of ~1:2 $Sr(NO_3)_2$:$NaNO_2$ in MeOH and H_2O and ESI-MS/MS spectra of b) $[Sr_2(NO_2)_2(NO_3)_3]^-$ (454 m/z), c) $[Sr_2(NO_2)_3(NO_3)_2]^-$ (438 m/z), d) $[Sr_2(NO_2)_4(NO_3)]^-$ (422 m/z), e) $[Sr(NO_2)(NO_3)_2]^-$ (258 m/z), f) $[Sr(NO_2)_2(NO_3)]^-$ (242 m/z), and g) $[Sr(NO_2)_3]^-$ (226 m/z).

CID of $[Sr_2(NO_2)_2(NO_3)_3]^-$ at 454 m/z results in the elimination of neutral $Sr(NO_2)_2$ (loss of 180 amu) to leave $[Sr(NO_3)_3]^-$ at 274 m/z. CID of $[Sr_2(NO_2)_3(NO_3)_2]^-$ at 438 m/z and $[Sr_2(NO_2)_4(NO_3)]^-$ at 422 m/z also results in the elimination of neutral $Sr(NO_2)_2$ to leave $[Sr(NO_2)(NO_3)_2]^-$ at 258 m/z and $[Sr(NO_2)_2(NO_3)]^-$ at 242 m/z, respectively, and suggests that Sr

strongly binds and preferentially retains NO_2^-. Subsequent CID of both $[Sr(NO_2)(NO_3)_2]^-$ at 258 m/z and $[Sr(NO_2)_2(NO_3)]^-$ at 242 m/z results in the formation of the bare nitrate anion, $[NO_3]^-$ at 62 m/z by elimination of neutral $Sr(NO_2)(NO_3)$ and $Sr(NO_2)_2$, respectively. The $[Sr(NO_2)_3]^-$ species at 226 m/z dissociates to leave the bare nitrite anion, $[NO_2]^-$ at 46 m/z by loss of neutral $Sr(NO_2)_2$, though the ESI-MS/MS spectra of $[Mn(NO_2)_3]^-$ and $[Zn(NO_2)_3]^-$ reported in an earlier study reveal multiple losses of NO as the dominant processes.(Fraſski, Osiſska and Gierczyk 2016) The sodium nitrite anion $[Na(NO_2)_2]^-$ was observed at 115 m/z, $[Na(NO_2)(NO_3)]^-$ at 131 m/z, and the sodium cluster $[Na_2(NO_2)_2(NO_3)]^-$ at 200 m/z. No attempts to further characterize the sodium complexes by ESI-MS/MS were made.

The positive ESI-MS spectrum (10-500 m/z) of a ~1:2 $Sr(NO_3)_2$:$NaNO_2$ in 50:50 (by volume) MeOH:H_2O is also shown in Figure 4 (bottom). The dominant product ion observed at 150 m/z is $[Sr(NO_3)]^+$. The ion at 134 m/z, assigned as $[Sr(NO_2)]^+$, is the second most abundant ion in the spectrum (60% relative abundance). Cationic strontium clusters were observed at 362, 346, 330, and 314 m/z, where the ions at 362 and 314 m/z are $[Sr_2(NO_3)_3]^+$ and $[Sr(NO_2)_3]^+$, respectively. The ions observed at 346 and 330 m/z are strontium clusters that contain a mixture of NO_3^- and NO_2^- ligands. The ion at 346 m/z is assigned a composition of $[Sr_2(NO_2)(NO_3)_2]^+$, and the ion at 330 m/z is assigned as $[Sr_2(NO_2)_2(NO_3)]^+$. Again, the variations in the relative abundances of the strontium cluster ions suggest competition between nitrate and nitrite for Sr binding. Still, the dominant species in the ESI-MS spectrum is $[Sr(NO_3)]^+$ and offers evidence that nitrate may outcompete nitrite for Sr binding to form ionic species but does not provide definitive insight as to whether nitrite is more competitive for Sr binding to form neutral species.

ESI-MS/MS spectra produced by CID of each of the cationic strontium nitrate/nitrite clusters can be found in Figure 6.

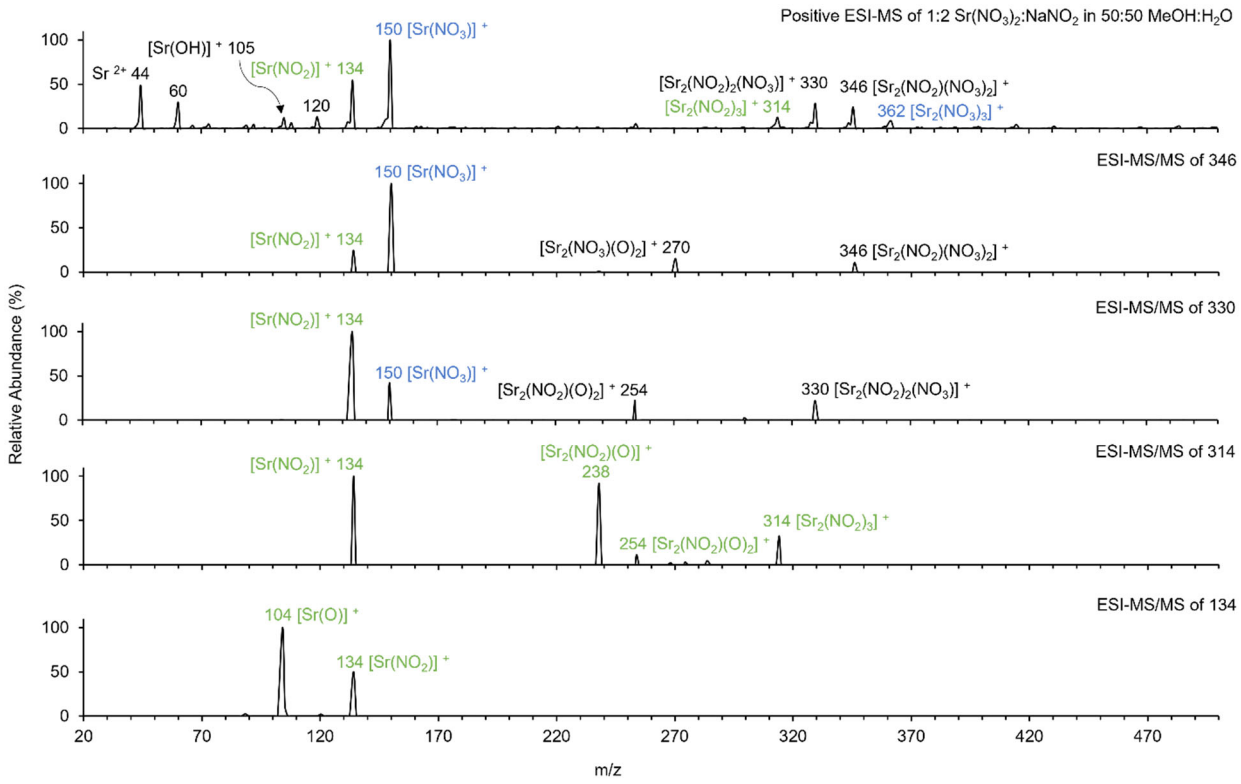

Figure 6. (Top to bottom) Positive a) ESI-MS of ~1:2 $Sr(NO_3)_2$:$NaNO_2$ in MeOH and H_2O and ESI-MS/MS spectra of b) $[Sr_2(NO_2)(NO_3)_2]^+$ (346 m/z), c) $[Sr_2(NO_2)_2(NO_3)]^+$ (330 m/z), d) $[Sr_2(NO_2)_3]^+$ (314 m/z), and e) $[Sr(NO_2)]^+$ (134 m/z).

CID of the $[Sr_2(NO_2)(NO_3)_2]^+$ precursor at 346 m/z reveals elimination of neutral $SrNO_2NO_3$ (loss of 196 amu) to leave $[Sr(NO_3)]^+$ as the dominant product. Modest amounts of $[Sr(NO_2)]^+$ at 134 m/z and an ion at 270 m/z were also observed. $[Sr(NO_2)]^+$ at 134 m/z reasonably forms by the elimination of neutral $Sr(NO_3)_2$ (loss of 212 amu), whereas the loss of 76 amu to form the ion at 270 m/z corresponds to a cumulative loss of NO_2 and NO. Conversely, CID of the $[Sr_2(NO_2)_2(NO_3)]^+$ precursor at 330 m/z yields $[Sr(NO_2)]^+$ at 134 m/z as the dominant product, $[Sr(NO_3)]^+$ at 150 m/z, and a minor product at 254 m/z. Formation of $[Sr(NO_2)]^+$ at 134 m/z and $[Sr(NO_3)]^+$ at 150 m/z occurs by loss of neutral $SrNO_2NO_3$ and $Sr(NO_2)_2$, respectively. Generation of the ion at 254 m/z involves the loss of 76 amu, presumably a cumulative loss of NO_2 and NO. CID of $[Sr_2(NO_2)_3]^+$ (314 m/z) leads primarily to the elimination of neutral $Sr(NO_2)_2$

(loss of 180 amu) to form $[Sr(NO_2)]^+$ at 134 m/z, along with the loss of 76 amu to generate the ion at 238 m/z, presumably by the cumulative loss of NO_2 and NO. Based on a comparison of the ESI-MS/MS spectra of $[Sr_2(NO_3)_3]^+$ (362 m/z), $[Sr_2(NO_2)(NO_3)_2]^+$ (346 m/z), $[Sr_2(NO_2)_2(NO_3)]^+$ (330 m/z), and $[Sr_2(NO_2)_3]^+$ (314 m/z), we anticipate that for $[Sr_2(NO_2)(NO_3)_2]^+$ (346 m/z) and $[Sr_2(NO_2)_2(NO_3)]^+$ (330 m/z) the loss of NO_2 may come from an $(NO_3)^-$ ligand, and the loss of NO may come from an $(NO_2)^-$ ligand. For $[Sr_2(NO_2)_3]^+$ (314 m/z), the loss of 76 amu to form the ion at 238 m/z can likely be attributed to the loss of an $(NO_2)^-$ ligand and loss of NO from a second $(NO_2)^-$ ligand. CID of $[Sr_2(NO_2)_3]^+$ at 314 m/z also yields the ion at 254 m/z by the loss of 60 amu, likely corresponding to the elimination of two NO molecules to leave $[Sr_2(NO_2)(O)_2]^+$. Subsequent CID of $[Sr(NO_2)]^+$ results in the elimination of NO to yield $[Sr(O)]^+$ at 104 m/z.

3.3 Competition of Nitrate and Hydroxide for Sr

The negative and positive ESI-MS spectra for 1:2 $Sr(NO_3)_2$:NH_4OH in 50:50 (by volume) MeOH:H_2O are superimposed upon the respective negative and positive ESI-MS spectra for

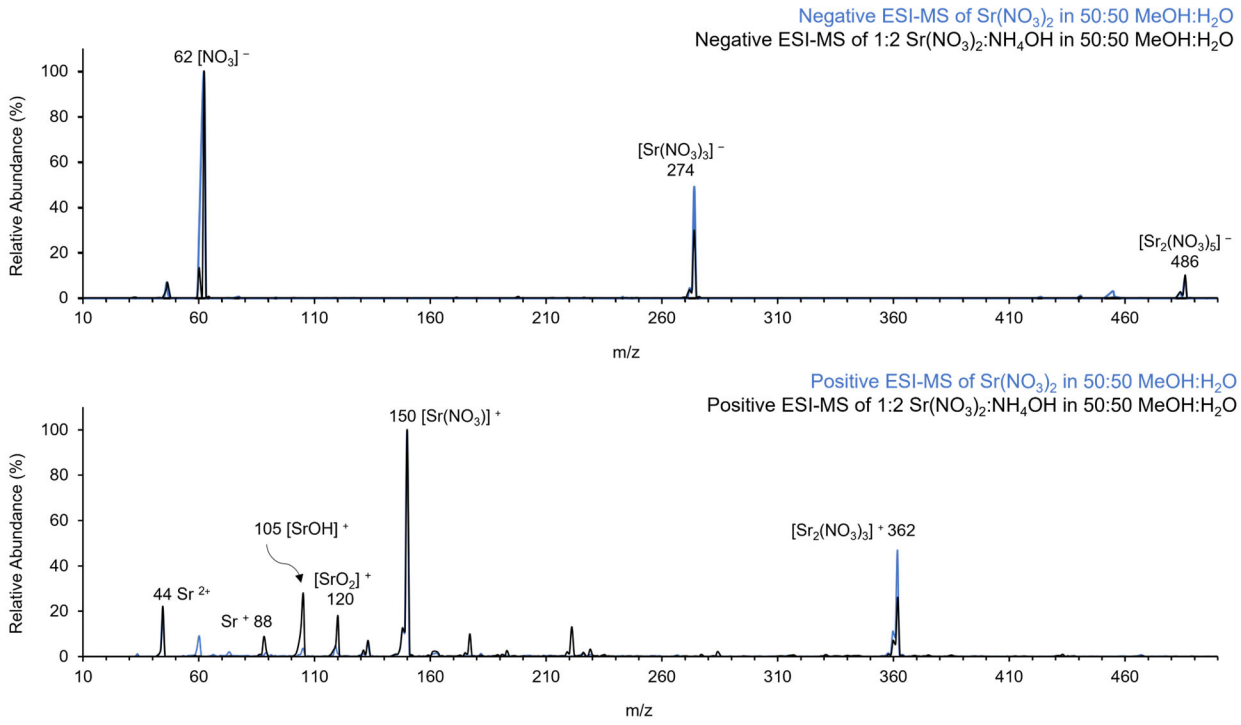

Figure 7. Negative (top) and positive (bottom) ESI-MS (10-500 m/z) of ~1:2 $Sr(NO_3)_2$:NH_4OH in MeOH and H_2O (black traces) are superimposed upon the respective negative and positive ESI-MS spectra for $Sr(NO_3)_2$ (blue traces) in MeOH and H_2O.

$Sr(NO_3)_2$ in MeOH and H_2O and displayed in Figure 7 (10-500 m/z). The anionic species observed are assigned as $[Sr_2(NO_3)_5]^-$ at 486 m/z, $[Sr(NO_3)_3]^-$ at 274 m/z, and $[NO_3]^-$ at 62 m/z. $[NO_3]^-$ is the dominant species in the negative ESI spectrum. Anions containing Sr and the OH^- moiety were not observed. The hydroxide anion, OH^- was not observed at 17 m/z. Cations observed in the positive ESI spectrum include $[Sr_2(NO_3)_3]^+$ at 362 m/z, $[Sr(NO_3)]^+$ at 150 m/z, presumably $[Sr(O_2)]^+$ at 120 m/z, $[SrOH]^+$ at 105 m/z, and bare Sr^+ and Sr^{2+} at 88 and 44 m/z, respectively. The $[Sr(NO_3)]^+$ peak at 150 m/z dominates the spectrum, and the relative abundance of $[SrOH]^+$ at 105 m/z is ~30% of the $[Sr(NO_3)]^+$ peak. A closer examination of the dissociation of NH_4^+ in the presence of MeOH and the preferential dissociation of NH_4OH to NH_3

and H_2O rather than NH_4^+ and OH^- offers an explanation for the reduced abundance of the $[SrOH]^+$ peak.(Paabo, Bates and Robinson 1966, Hawkes 2004) More specifically, the suppressed production of OH^- results in a limited availability of free OH^- to bind Sr^{2+}.

The competition of NO_3^- and OH^- for Sr binding was reassessed by preparing a ~1:2 $Sr(NO_3)_2$:NaOH solution in 50:50 (by volume) MeOH:H_2O and examining the resulting negative and positive ESI-MS spectra, shown in Figure 8. The dominant anion observed is $[NO_3]^-$ at 62

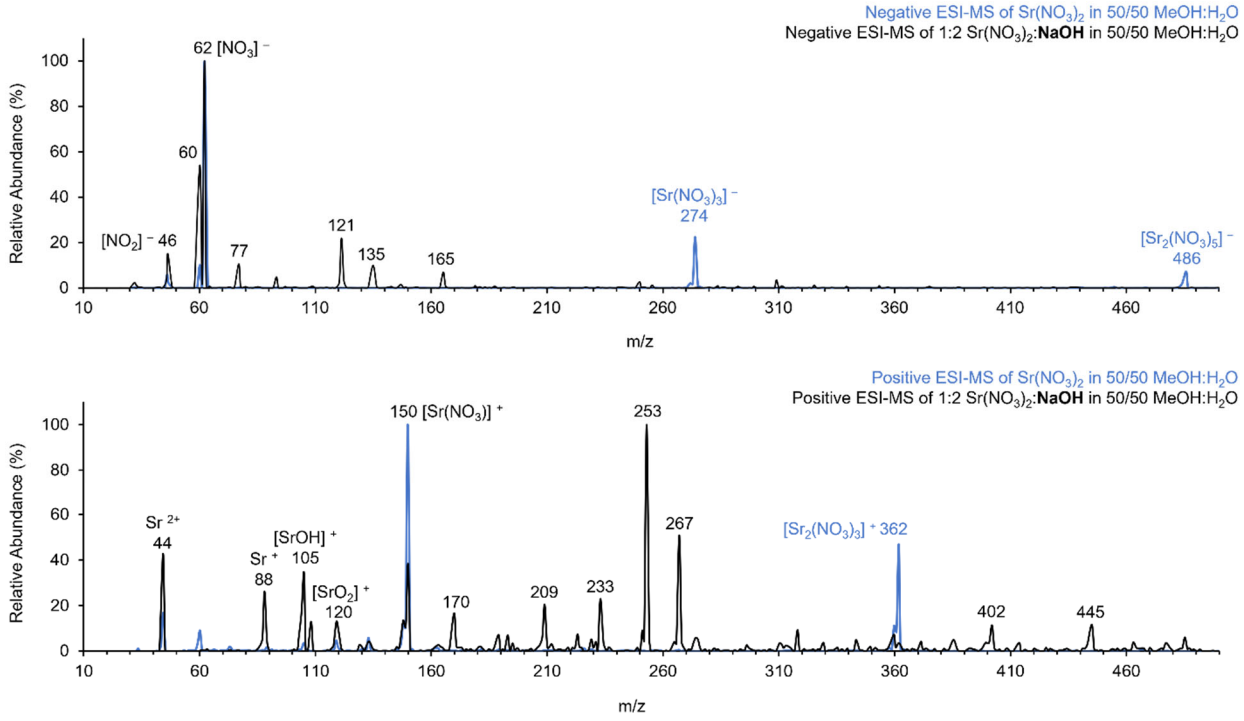

Figure 8. Negative (top) and positive (bottom) ESI-MS (10-500 m/z) of ~1:2 $Sr(NO_3)_2$:NaOH in MeOH and H_2O (black traces) are superimposed upon the respective negative and positive ESI-MS spectra for $Sr(NO_3)_2$ (blue traces) in MeOH and H_2O.

m/z, which is consistent with the negative ESI-MS spectrum of the ~1:2 $Sr(NO_3)_2$:NH_4OH solution. The hydroxide anion was not observed. Interestingly, no anionic species containing Sr and NO_3^- were observed. Anionic species containing Sr and OH^- were not observed either. It is possible that Na introduced by using NaOH as the OH^- donor is more competitive than Sr for nitrate and hydroxide complexation. An alternative explanation may also be that formation of the neutral species is the dominant process, but this cannot be determined solely using ESI-MS.

The relevant cations observed in the positive ESI-MS spectrum include Sr^{2+} at 44 m/z, Sr^{+} at 88 m/z, $[SrOH]^{+}$ at 105 m/z, and $[Sr(NO_3)]^{+}$ at 150 m/z. The relative abundances of these ions can be used to assess the competition of NO_3^- and OH^- for Sr^{2+}. The $[SrOH]^{+}$ and $[Sr(NO_3)]^{+}$ ions are observed in nearly equal relative abundances (~ 40%); however, the relative abundances of the bare Sr^{2+} and Sr^{+} cations (44 and 88 m/z respectively) are greater than those observed in the positive ESI-MS spectrum of the ~1:2 $Sr(NO_3)_2$:NH_4OH solution and suggest that Na competes with Sr for NO_3^- and OH^- binding. Bare Na^{+} was not observed at 23 m/z and supports the hypothesis that there is competition between Na and Sr for ligand binding.

3.4 Competition of Nitrate and Chloride for Sr

The negative and positive ESI-MS spectra (20-500 m/z) of ~1:1 $Sr(NO_3)_2$:$SrCl_2$ in 50:50 (by volume) MeOH:H_2O are shown in Figure 9.

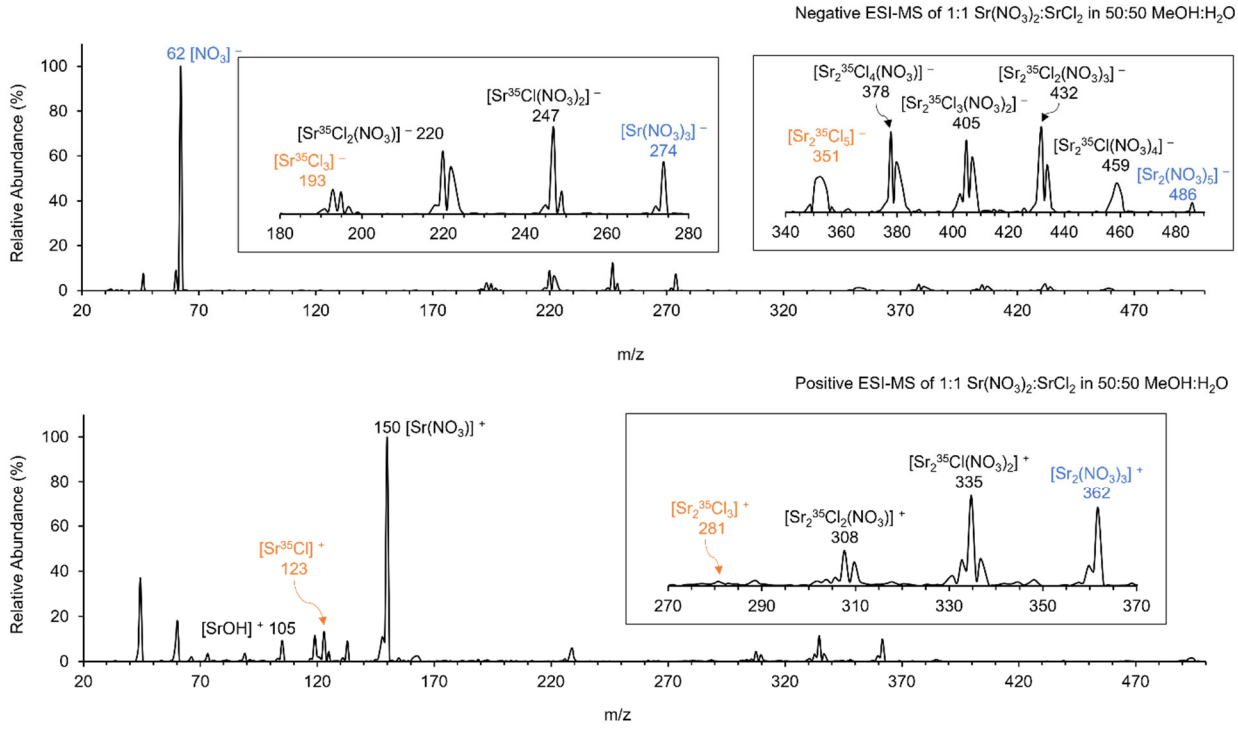

Figure 9. Negative (top) and positive (bottom) ESI-MS spectra (20-500 m/z) of ~1:1 $Sr(NO_3)_2$:$SrCl_2$ in MeOH and H_2O. Inset spectra are included to show ions containing Sr complexed to a mixture of nitrate and chloride ligands more clearly.

The bare nitrate anion at 62 m/z dominates the spectrum of the 1:1 mixture of $Sr(NO_3)_2$:$SrCl_2$. Other product ions observed include $[Sr(NO_3)_3]^-$ at 274 m/z and $[SrCl_3]^-$ at 193 m/z, along with ionic Sr species that contain a mixture of NO_3^- and Cl^- ligands at 247 and 220 m/z. The compositions of the ions at 247 and 220 m/z are assigned as $[SrCl(NO_3)_2]^-$ and $[SrCl_2(NO_3)]^-$, respectively. Anionic Sr clusters containing nitrate and chloride ligands were also observed at 486, 459, 432, 405, 378, and 351 m/z. These species are assigned as $[Sr_2(NO_3)_5]^-$, $[Sr_2Cl(NO_3)_4]^-$, $[Sr_2Cl_2(NO_3)_3]^-$, $[Sr_2Cl_3(NO_3)_2]^-$, $[Sr_2Cl_4(NO_3)]^-$, and $[Sr_2Cl_5]^-$, respectively. Clusters of isotopic peaks are observed for chloride-containing species and correspond to ^{35}Cl and ^{37}Cl isotopic relative abundances (~75/25, respectively), consistent with natural isotopic ratios.

The negative ESI-MS/MS spectra of the mixed Sr nitrate/chloride species contained within the ESI spectrum of ~1:1 $Sr(NO_3)_2$:$SrCl_2$ in 50:50 (by volume) MeOH:H_2O are shown in Figure 10.

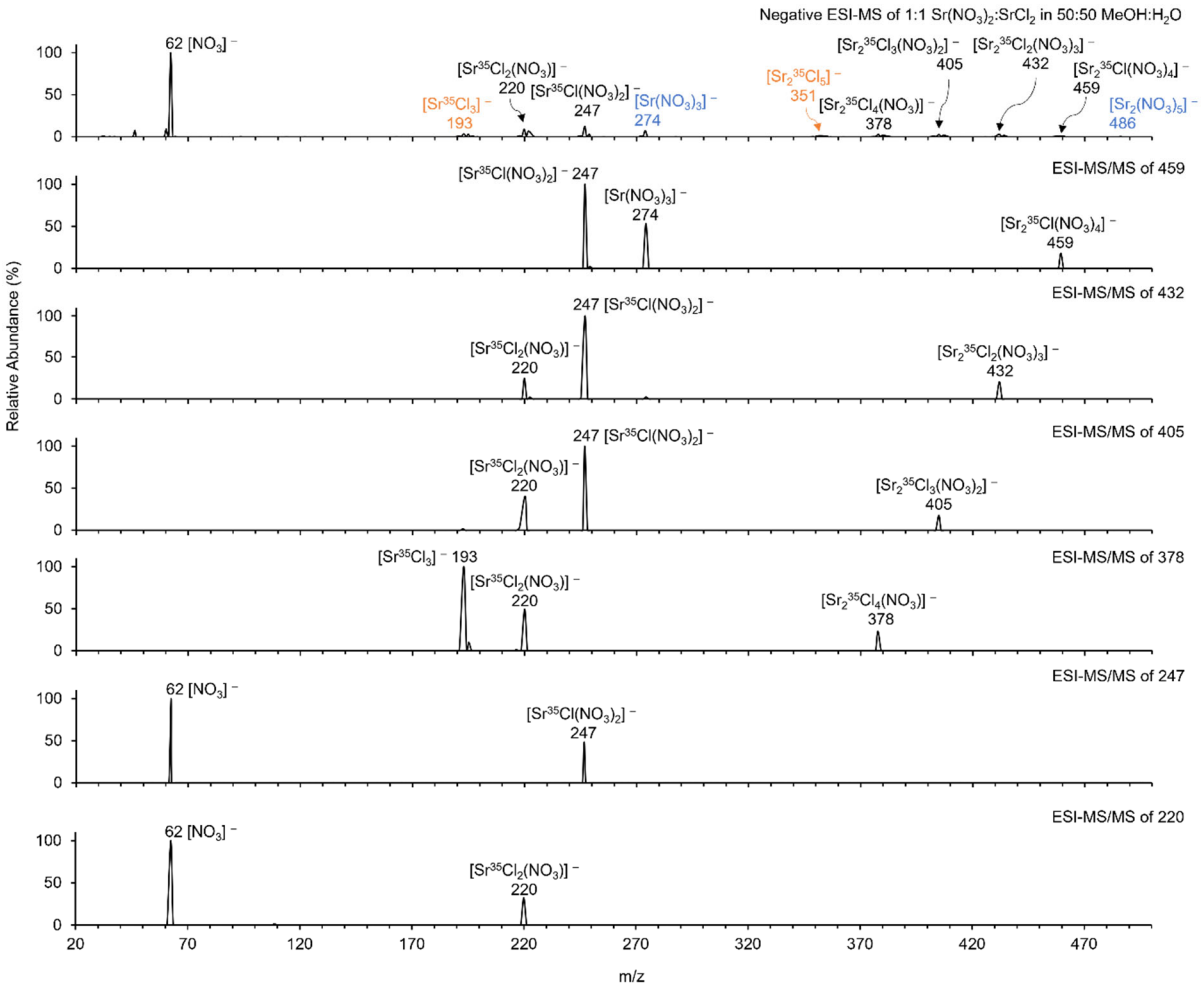

Figure 10. (Top to bottom) Negative a) ESI-MS spectrum (20-500 m/z) of ~1:1 $Sr(NO_3)_2$:$SrCl_2$ in MeOH and H_2O and ESI-MS/MS spectra of b) $[Sr_2{}^{35}Cl(NO_3)_4]^-$ (459 m/z), c) $[Sr_2{}^{35}Cl_2(NO_3)_3]^-$ (432 m/z), d) $[Sr_2{}^{35}Cl_3(NO_3)_2]^-$ (405 m/z), e) $Sr_2{}^{35}Cl_4(NO_3)]^-$ (378 m/z), f) $[Sr^{35}Cl(NO_3)_2]^-$ (247 m/z), and g) $[Sr^{35}Cl_2(NO_3)]^-$ (220 m/z).

CID of $[Sr_2{}^{35}Cl(NO_3)_4]^-$ at 459 m/z results in the elimination of neutral $Sr(NO_3)_2$ to form the dominant $[Sr^{35}Cl(NO_3)_2]^-$ product at 247 m/z and elimination of neutral $Sr^{35}Cl(NO_3)$ to form $[Sr(NO_3)_3]^-$ at 274 m/z. $[Sr_2{}^{35}Cl_2(NO_3)_3]^-$ at 432 m/z also eliminates $Sr^{35}Cl(NO_3)$ and $Sr(NO_3)_2$ to form $[Sr^{35}Cl(NO_3)_2]^-$ at 247 m/z and $[Sr^{35}Cl(NO_3)]^-$ at 220 m/z. CID of the $[Sr_2{}^{35}Cl_3(NO_3)_2]^-$

cluster at 405 m/z yields $[Sr^{35}Cl(NO_3)_2]^-$ by loss of neutral $SrCl_2$ and $[Sr^{35}Cl_2(NO_3)]^-$ by loss of neutral $SrCl(NO_3)$. The $[Sr_2{}^{35}Cl_4(NO_3)]^-$ cluster at 378 m/z also eliminates $SrCl_2$ and $SrCl(NO_3)$ to yield $[Sr^{35}Cl_2(NO_3)]^-$ at 220 m/z and $[Sr^{35}Cl_3]^-$ at 193 m/z, respectively. $[Sr^{35}Cl(NO_3)_2]^-$ at 247 m/z and $[Sr^{35}Cl_2(NO_3)]^-$ at 220 m/z both dissociate to leave the bare nitrate anion, $[NO_3]^-$ at 62 m/z.

The positive ESI-MS spectrum (20-500 m/z) of ~1:1 $Sr(NO_3)_2$:$SrCl_2$ in 50:50 (by volume) MeOH:H_2O shows $[Sr(NO_3)]^+$ as the dominant cation. $[SrCl]^+$ at 123 m/z is also observed, though its relative abundance is < 20% of the $[Sr(NO_3)]^+$ peak, suggesting that NO_3^- is more competitive than Cl^- to bind Sr^{2+}. Cationic strontium clusters containing multiple chloride and nitrate ligands are observed at 362, 335, 308, and 281 m/z. The compositions of these ions are assigned as $[Sr_2(NO_3)_3]^+$, $[Sr_2Cl(NO_3)_2]^+$, $[Sr_2Cl_2(NO_3)]^+$, and $[Sr_2Cl_3]^+$, respectively. The ESI-MS/MS spectra for $[Sr_2Cl(NO_3)_2]^+$ and $[Sr_2Cl_2(NO_3)]^+$ can be found in Figure 11.

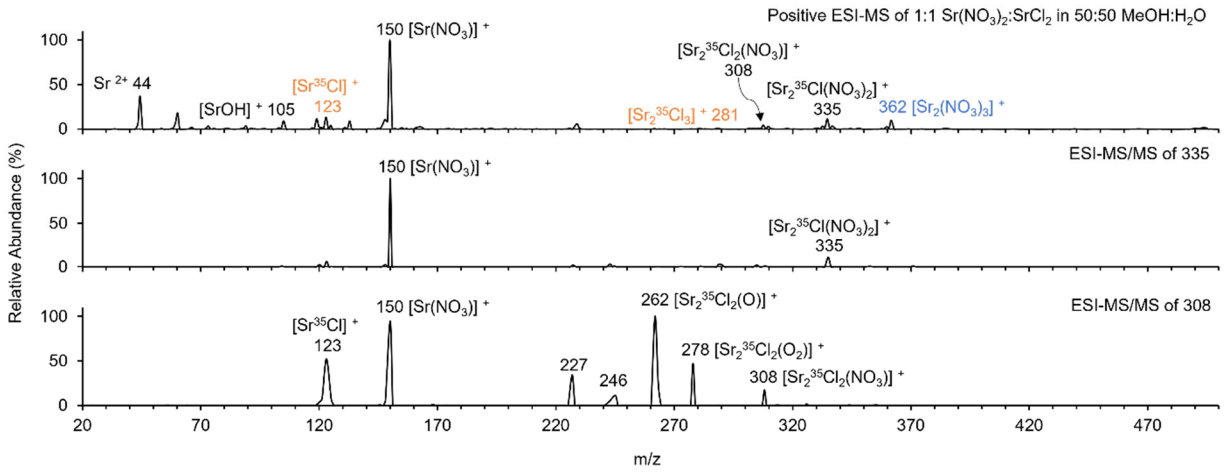

Figure 11. (Top to bottom) Positive a) ESI-MS spectrum (20-500 m/z) of ~1:1 $Sr(NO_3)_2$:$SrCl_2$ in MeOH and H_2O and ESI-MS/MS spectra of b) $[Sr_2{}^{35}Cl(NO_3)_2]^+$ (335 m/z), and c) $[Sr_2{}^{35}Cl_2(NO_3)]^+$ (308 m/z).

CID of $[Sr_2{}^{35}Cl(NO_3)_2]^+$ at 335 m/z results in the elimination of neutral $SrCl(NO_3)$ to form $[Sr(NO_3)]^+$. Conversely, CID of $[Sr_2{}^{35}Cl_2(NO_3)]^+$ results in the production of several product ions.

The most abundant product ions are observed at 262, 150, and 123 m/z, corresponding to compositions of $[Sr^{35}Cl_2(O)]^+$, $[Sr(NO_3)]^+$, and $[Sr^{35}Cl]^+$, respectively.

The negative and positive ESI mass spectra of the 1:1 $Sr(NO_3)_2$:$SrCl_2$ mixture superimposed upon the respective negative and positive ESI-MS spectra of the individual $Sr(NO_3)_2$ and $SrCl_2$ ESI solutions can be found in Figure 12.

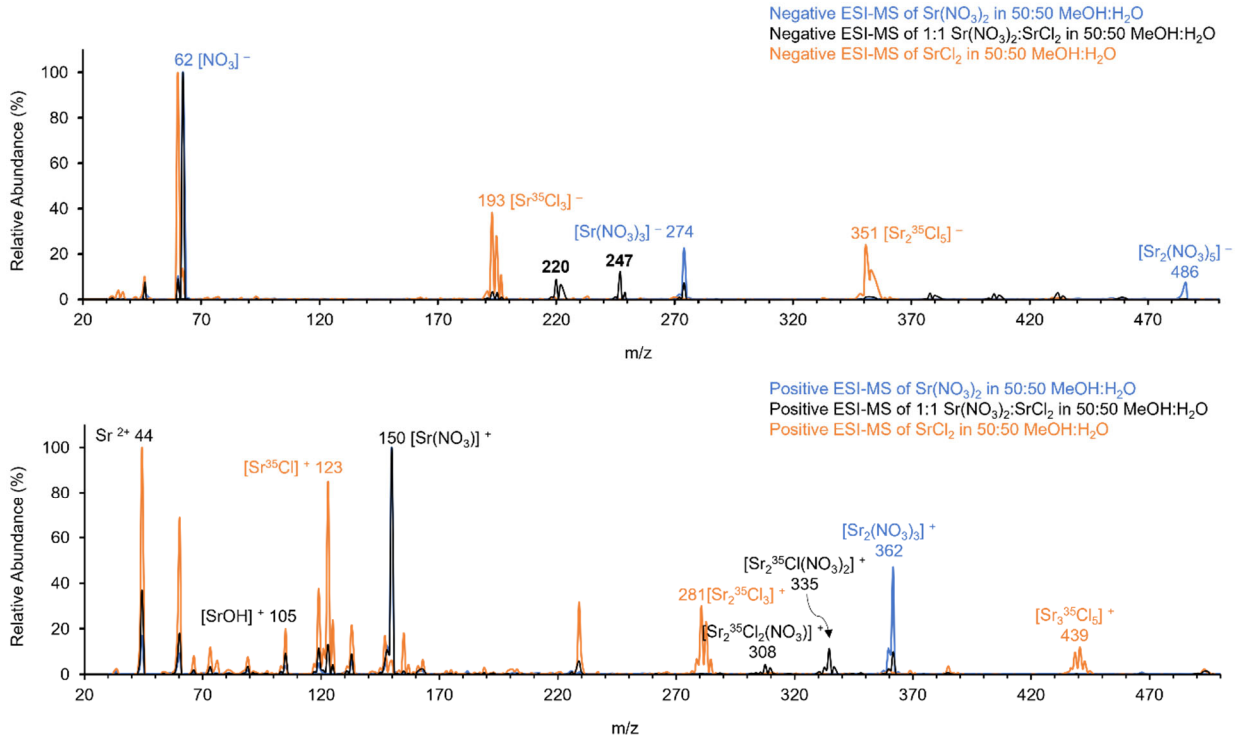

Figure 12. Negative (top) and positive (bottom) ESI-MS spectra (20-500 m/z) of ~1:1 $Sr(NO_3)_2$:$SrCl_2$ in MeOH and H_2O superimposed upon the respective negative and positive ESI-MS spectra of the individual $Sr(NO_3)_2$ (blue trace) and $SrCl_2$ (orange trace) ESI solutions.

3.5 Competition of Nitrate, Nitrite, Hydroxide, and Chloride for Sr

The negative and positive ESI-MS spectra for ~1:2:2:1 $Sr(NO_3)_2$:$NaNO_2$:NH_4OH:$SrCl_2$ in 50:50 (by volume) MeOH:H_2O are shown in Figure 13.

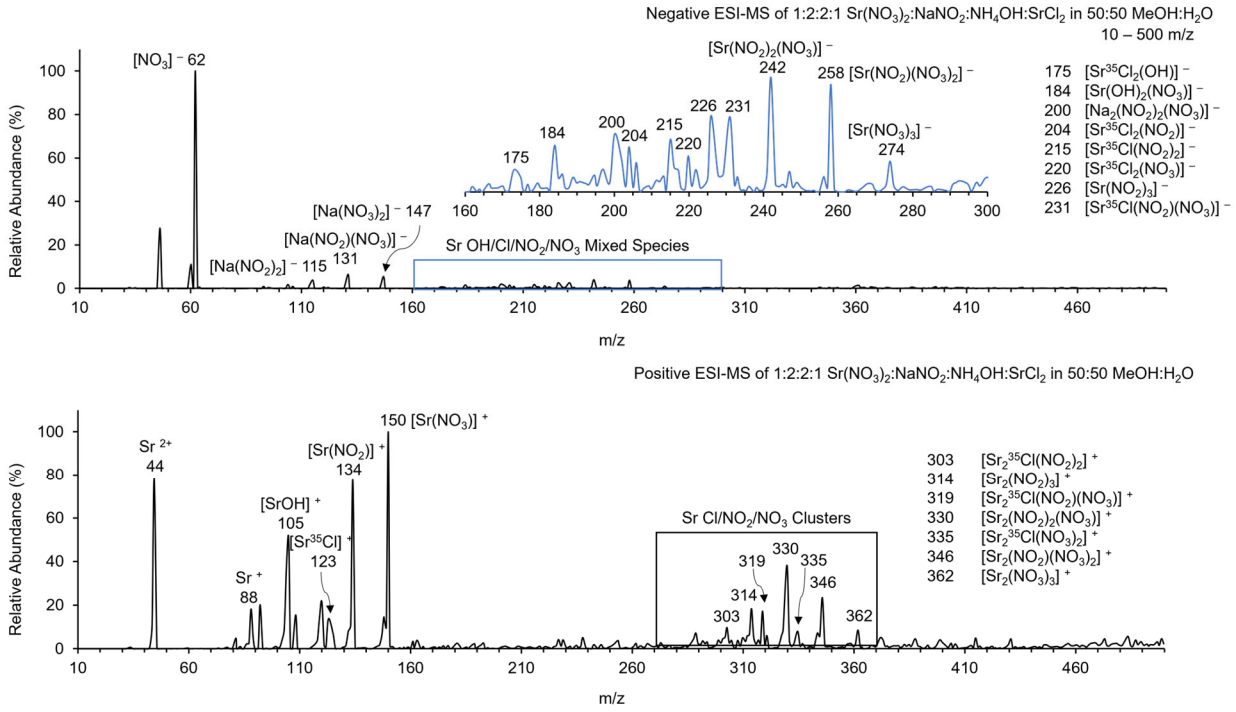

Figure 13. The negative (top) and positive (bottom) ESI-MS spectra for ~1:2:2:1 $Sr(NO_3)_2$:$NaNO_2$:NH_4OH:$SrCl_2$ (so that concentrations of the complexing anions are ~1:1:1:1) in MeOH and H_2O.

Proportions of $NaNO_2$ and NH_4OH were doubled so that the ratio of the concentrations of the complexing anions, NO_3^-, NO_2^-,OH^-, and Cl^- was ~1:1:1:1. The most abundant product observed in the negative ESI spectrum (Figure 13, top) is the bare nitrate anion at 62 m/z. Small amounts of the sodium nitrite/nitrate species $[Na(NO_2)_2]^-$, $[Na(NO_2)(NO_3)]^-$, and $[Na(NO_3)_2]^-$ were also observed at 115, 131, and 147 m/z, respectively. Several anionic Sr species including a mixture of the complexing anions were also observed. The most abundant Sr-containing species observed were $[Sr(NO_2)_2(NO_3)]^-$ at 242 m/z and $[Sr(NO_2)(NO_3)_2]^-$ at 258 m/z. The relative abundances of the anionic Sr species observed suggest that NO_3^- and NO_2^- are strong competitors to bind Sr^{2+}.

The most abundant ion observed in the positive ESI spectrum is $[Sr(NO_3)]^+$ at 150 m/z followed by $[Sr(NO_2)]^+$ at 134 m/z (~80% relative abundance). $[SrOH]^+$ at 105 m/z is also

observed, though only with ~50% relative abundance. A smaller amount (~15% relative abundance) of $[Sr^{35}Cl]^+$ at 123 m/z is observed. Sr clusters containing a mixture of chloride, nitrite and nitrate ligands were also observed and are shown in Figure 13 (bottom). The most abundant of these clusters are $[Sr_2(NO_2)_2(NO_3)]^+$ at 330 m/z and $[Sr_2(NO_2)(NO_3)_2]^+$ at 346 m/z. Again, the observation of mixed strontium nitrate/nitrite cluster ions indicates that NO_3^- and NO_2^- are highly competitive for Sr binding. Cationic strontium clusters containing OH^- were not readily observed, and the relative abundances of Sr clusters containing Cl^- were lower than those containing NO_3^- and NO_2^-.

The competition of NO_3^-, NO_2^-, OH^-, and Cl^- for Sr binding was reassessed by preparing a ~1:2:2:1 $Sr(NO_3)_2$:$NaNO_2$:NaOH:$SrCl_2$ in 50:50 (by volume) MeOH:H_2O and examining the resulting negative and positive ESI-MS spectra, shown in Figure 14.

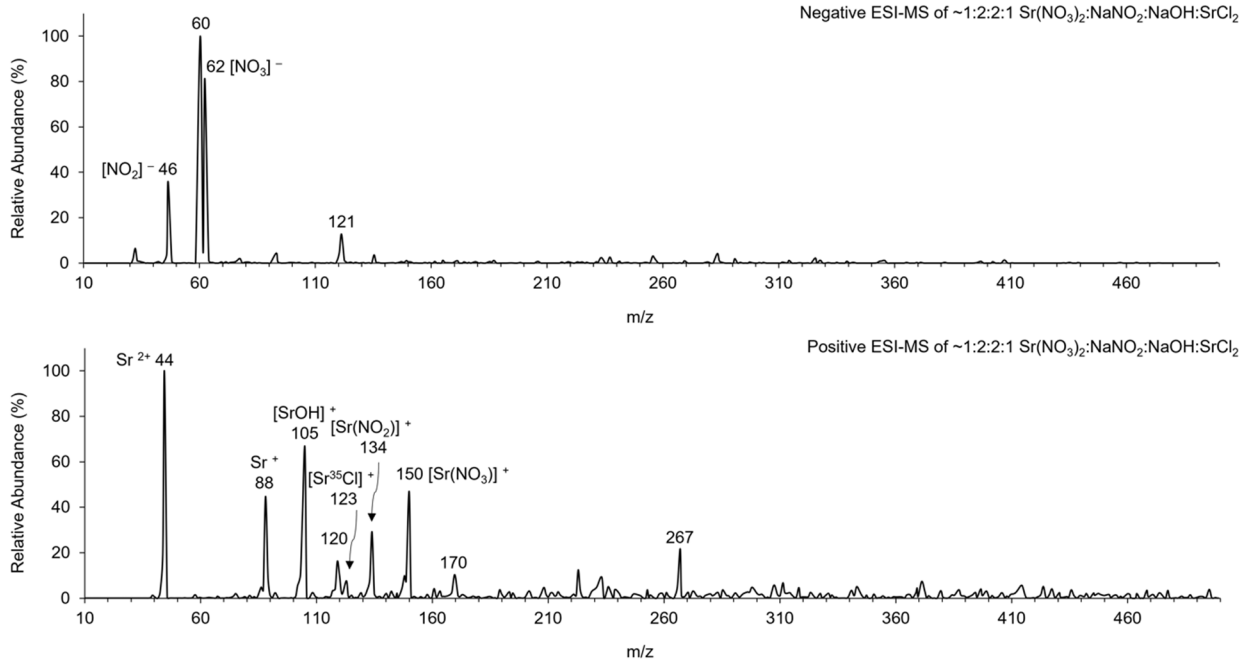

Figure 14. The negative (top) and positive (bottom) ESI-MS spectra for ~1:2:2:1 $Sr(NO_3)_2$:$NaNO_2$:NaOH:$SrCl_2$ (so that concentrations of the complexing anions are ~1:1:1:1) in MeOH and H_2O.

These spectra display more noise that is attributed to dilution of the spray solution by a factor of 10 (needed to overcome issues associated with salt crystallization and clogging of the ESI

needle brought on presumably by increased Na concentration). The ions observed in the negative ESI-MS spectrum using the ~1:2:2:1 $Sr(NO_3)_2$:$NaNO_2$:NaOH:$SrCl_2$ in 50:50 (by volume) MeOH:H_2O include $[NO_2]^-$ and $[NO_3]^-$ at 46 and 62 m/z, respectively. The ion at 60 m/z was observed in all negative ESI-MS spectra presented in this study and is attributed to the MeOH:H_2O solvent, but the peak at 60 m/z is more pronounced in the negative ESI-MS spectrum shown in Figure 14 presumably because of the decreased concentration of the analytes of interest used in the spray solution. The positive ESI-MS spectrum produced using the ~1:2:2:1 $Sr(NO_3)_2$:$NaNO_2$:NaOH:$SrCl_2$ in 50:50 (by volume) MeOH:H_2O spray solution is shown in Figure 14, bottom. The most abundant ion observed is Sr^{2+} at 44 m/z. Other strontium-containing cations observed include Sr^+, $[SrOH]^+$, $[Sr(NO_2)]^+$, and $[Sr(NO_3)]^+$ at 88, 105, 134, and 150 m/z, respectively, and a small amount (< 10% relative abundance) of $[Sr^{35}Cl]^+$ was observed at 123 m/z. Cationic strontium clusters are not readily distinguished from the noise in the spectrum. Competition between each of the complexing anions for Sr binding can be assessed by examining the relative abundances of the complexed strontium species. The most abundant Sr-containing species in the positive ESI-MS spectrum is $[SrOH]^+$ (~ 70% of the Sr^{2+} peak) followed by $[Sr(NO_3)]^+$ (~ 50%) and $[Sr(NO_2)]^+$ (~ 30%). Interestingly, the relative abundances of bare Sr^{2+} and Sr^+ are greater when using NaOH instead of NH_4OH as the OH^- donor in the spray solution and suggests that Na competes with Sr for ligand binding. The relative abundance of $[SrOH]^+$ is greater when using NaOH (~ 70%) instead of NH_4OH (~50%) presumably because more OH^- is available from the dissociation of NaOH to Na^+ and OH^- than from the dissociation of NH_4OH (which dissociates primarily to NH_3 and H_2O rather than NH_4^+ and OH^-). Overall, the results show that OH^-, NO_3^-, and NO_2^- are strong competitors for Sr^{2+} binding.

4.0 Relevance to Hanford Tank Waste Separations

The CST ion exchange media utilized in the tank side cesium removal process is selective for Cs and has also been shown to effectively remove the group II metals Ca, Sr, and Ba from both simulant and actual Hanford tank waste.(Fiskum, Rovira et al. 2019, Fiskum, Campbell and Trang-Le 2020, Campbell, Westesen et al. 2021, Fiskum, Campbell et al. 2021, Fiskum, Westesen et al. 2021, Westesen, Campbell et al. 2022) Despite the high selectivity of CST for Cs, the distribution ratio for Sr is nearly twice that for Cs, suggesting that CST may preferentially bind Sr. In some instances, Sr is nearly quantitatively removed and retained by the CST ion exchange media while in others, the Sr is recovered in the effluent. $[SrOH]^+$ was initially suspected to be the adsorbed species,(Hamm 2004) although additional investigation refuted this hypothesis.(Fiskum, Campbell and Trang-Le 2020) Developing an understanding of Sr speciation in complex tank waste matrices is important to improve ongoing high level waste separation and immobilization efforts as well as to predict the transport and fate of Sr in nuclear waste processing schemes.

The present ESI-MS results reveal that OH^-, NO_3^- and NO_2^- are highly competitive complexing agents available to form soluble Sr species in Hanford tank waste. ESI-MS may offer qualitative and quantitative stoichiometric information that is likely to correlate with solution phase chemistry.(Glish and Vachet 2003, Schröder 2012) The solution-phase conditions that may not necessarily be reflected in ESI-MS studies include changes in concentration, pH, and solvation,(Kebarle and Verkerk 2009) and some detected species may be more easily observed or exclusive to gas phase studies (due to the instability of some oxidation states in solution). Nevertheless, the present results show that Sr^{2+} complexes with OH^-, NO_3^-, NO_2^-, and Cl^- to form $[SrOH]^+$, $[Sr(NO_3)]^+$, $[Sr(NO_2)]^+$, and $[SrCl]^+$ along with several cationic clusters that include combinations of NO_3^-, NO_2^-, and Cl^- ligands. Because ion exchange studies have indicated that $[SrOH]^+$ is not the dominant species affecting current tank side cesium removal processing

schemes,(Fiskum, Campbell and Trang-Le 2020) the persistent formation of $[Sr(NO_3)]^+$ and $[Sr(NO_2)]^+$ in the present study suggests that these species may form in reasonable abundances within the Hanford tank wastes and may influence the ability to separate Sr in tank waste processing schemes utilizing the CST ion exchange media. The formation of such species may have implications in the ability to separate and retain Sr using CST ion exchange media in the tank side cesium removal process.

5.0 Conclusion

CST ion exchange media currently employed in the Hanford tank side cesium removal process is selective for Cs and displays a high selectivity and affinity for Sr in both tank waste simulants and actual Hanford tank waste. A better understanding of the speciation of Sr in tank waste media is important to predict the transport and fate of Sr in nuclear waste processing systems. The present ESI-MS results show that Sr^{2+} binds with NO_3^-, NO_2^-, OH^-, and Cl^-. Ion-exchange studies have concluded that $[SrOH]^+$ is not the dominant Sr species of concern in the tank side cesium removal process;(Fiskum, Campbell and Trang-Le 2020) however, $[Sr(NO_3)]^+$ and $[Sr(NO_2)]^+$ species may also form and affect the ability to separate Sr using CST in nuclear waste separation processes.

6.0 Ongoing Work and Future Directions

6.1 Part of West Area Risk Management (WARM) Project

Additional batch contact tests are being performed to independently assess the effect of NO_3^- and NO_2^- concentration upon the uptake of Sr by CST. The previous batch contact tests involved varying the concentration of OH^- and were used to determine that $SrOH^+$ was not the dominant Sr species.(Fiskum, Campbell and Trang-Le 2020) The ongoing batch contact test are also anticipated to assess the variation in uptake of known Sr species by CST.

6.2 ESI-MS Experiments

6.2.1 Competition Assessments

The nitrate, nitrite, and chloride salts of Sr are soluble, and the hydroxide salt of Sr is moderately soluble in aqueous media. The composition of tank waste also includes carbonate, sulfate, and phosphate, and although these salts of Sr have limited solubility in aqueous environments, carbonate is present in sufficient quantities in tank waste that it is worthwhile to also assess the competition between nitrate and carbonate for Sr binding. The results from the present study also suggest that Na and Sr compete for complexing agents, therefore a more detailed assessment of Na and Sr competition is warranted. Additional ESI-MS experiments will be conducted to assess the competition between NO_3^- and CO_3^{2-} for Sr binding, and to test the competition between Na and Sr for complexing anions.

6.2.2 Effect of pH upon the Observed Mass Spectrum

Previous reports have shown that pH can influence the ions observed in the mass spectrum. The pH values of the sample solutions in this study were in the range of 4-7. The alkaline conditions of tank waste are likely to be better represented by solutions with a pH > 7.

In future work, the pH of the sample solutions will be increased, and the mass spectra of the alkaline solutions will be compared to those collected in the present study to evaluate the effect of pH upon the observed speciation of Sr. Ion intensities and, therefore, relative abundances are expected to vary; however, the species observed are anticipated to remain consistent with those identified here.

6.2.3 Quantitative Analysis

The potential for ESI-MS to provide quantitative information is still being explored. The feasibility, limit of detection, and limit of quantification have not been established for the ESI-MS instrument used in the present study. Ion intensities and relative abundances of the detected ionic species are readily observed in the ESI spectrum, but it is unclear if ion intensities can be used to determine concentration in solution. Other factors such as ion source conditions and ionization efficiency of the analyte may influence the observed ion intensity more so than concentration of the analyte in the spray solution. Additional work involving several different analytes is crucial for an adequate assessment of the quantitative capabilities of the instrument.

6.3 Analysis by Inductively Coupled Plasma Mass Spectrometry

Inductively coupled plasma mass spectrometry (ICP-MS) is advantageous for quantitative elemental analysis. Due to the harsh conditions of the ICP ionization process, samples are atomized, and chemical speciation is not preserved. ICP-MS is routinely used for trace analysis and quantification and may be useful to detect Sr and other elements not retained by CST. Samples of the column eluent from AW-105 processing will be used for analysis.

7.0 References

Bubas, A. R., E. Perez, L. J. Metzler, S. D. Rissler and M. J. Van Stipdonk (2021). "Collision-induced dissociation of [UO2 (NO3) 3]− and [UO2 (NO3) 2 (O2)]− and reactions of product ions with H2O and O2." Journal of Mass Spectrometry **56**(3): e4705.

Bubas, A. R., I. J. Tatosian, A. Iacovino, T. A. Corcovilos and M. J. van Stipdonk (2024). "Reactions of gas-phase uranyl formate/acetate anions: reduction of carboxylate ligands to aldehydes by intra-complex hydride attack." Physical Chemistry Chemical Physics **26**(16): 12753-12763.

Campbell, E. L., A. M. Westesen, F. C. Colon, D. Boglaienko, T. G. Levitskaia and R. A. Peterson (2021). "Elemental characterization of crystalline silicotitanate following Hanford tank waste processing." Separation Science and Technology **56**(8): 1457-1465.

Colburn, H. A. and R. A. Peterson (2021). "A history of Hanford tank waste, implications for waste treatment, and disposal." Environmental Progress & Sustainable Energy **40**(1): e13567.

Fenn, J. B., M. Mann, C. K. Meng, S. F. Wong and C. M. Whitehouse (1989). "Electrospray ionization for mass spectrometry of large biomolecules." Science **246**(4926): 64-71.

Fenn, J. B., M. Mann, C. K. Meng, S. F. Wong and C. M. Whitehouse (1990). "Electrospray ionization–principles and practice." Mass Spectrometry Reviews **9**(1): 37-70.

Fiskum, S. K., E. L. Campbell, R. A. Peterson and T. L. Trang-Le (2021). Cesium Exchange onto Crystalline Silicotitanate from Blended Hanford Tank Wastes, Pacific Northwest National Lab.(PNNL), Richland, WA (United States).

Fiskum, S. K., E. L. Campbell and T. T. Trang-Le (2020). Crystalline Silicotitanate Batch Contact Testing with Ba, Ca, Pb, and Sr, Pacific Northwest National Lab.(PNNL), Richland, WA (United States).

Fiskum, S. K., A. M. Rovira, H. A. Colburn, A. M. Carney and R. A. Peterson (2019). Cesium ion exchange testing using a three-column system with crystalline silicotitanate and Hanford tank waste 241-AP-107, Pacific Northwest National Lab.(PNNL), Richland, WA (United States).

Fiskum, S. K., A. M. Westesen, A. M. Carney, T. T. Trang-Le and R. A. Peterson (2021). Ion exchange processing of AP-105 Hanford tank waste through crystalline silicotitanate in a staged 2-then 3-column system, Pacific Northwest National Lab.(PNNL), Richland, WA (United States).

Frański, R. (2015). "Mass spectrometric decomposition of [MNO3]+ cations, where M= Ca, Sr, Ba." Polyhedron **91**: 136-140.

Frański, R., K. Sobieszczuk and B. Gierczyk (2014). "Mass spectrometric decomposition of [Mn+ (NO3−) n+ 1]− anions originating from metal nitrates M (NO3) n." International Journal of Mass Spectrometry **369**: 98-104.

Fraſski, R., K. Osiſska and B. Gierczyk (2016). "Nitrite and nitrate anions as oxygen donors in the gas phase." International Journal of Mass Spectrometry **408**: 51-55.

Glish, G. L. and R. W. Vachet (2003). "The basics of mass spectrometry in the twenty-first century." Nature Reviews Drug Discovery **2**(2): 140-150.

Hamm, L. L. (2004). Preliminary Ion Exchange Modeling for Removal of Cesium from Hanford Waste Using Hydrous Crystalline Silicotitanate Material, Savannah River Site (SRS), Aiken, SC (United States).

Hawkes, S. J. (2004). "The formula for ammonia monohydrate." Journal of Chemical Education **81**(11): 1569.

Kebarle, P. and U. H. Verkerk (2009). "Electrospray: from ions in solution to ions in the gas phase, what we know now." Mass Spectrometry Reviews **28**(6): 898-917.

Leavitt, C. M., J. Oomens, R. P. Dain, J. Steill, G. S. Groenewold and M. J. Van Stipdonk (2009). "IRMPD spectroscopy of anionic group II metal nitrate cluster ions." Journal of the American Society for Mass Spectrometry **20**: 772-782.

Li, F., M. A. Byers and R. Houk (2003). "Tandem mass spectrometry of metal nitrate negative ions produced by electrospray ionization." Journal of the American Society for Mass Spectrometry **14**(6): 671-679.

McMahon, T. and P. Kebarle (1977). "Intrinsic acidities of substituted phenols and benzoic acids determined by gas-phase proton-transfer equilibriums." Journal of the American Chemical Society **99**(7): 2222-2230.

Oomens, J., L. Myers, R. Dain, C. Leavitt, V. Pham, G. Gresham, G. Groenewold and M. Van Stipdonk (2008). "Infrared multiple-photon photodissociation of gas-phase group II metal-nitrate anions." International Journal of Mass Spectrometry **273**(1-2): 24-30.

Paabo, M., R. G. Bates and R. Robinson (1966). "Dissociation of ammonium ion in methanol-water solvents." The Journal of Physical Chemistry **70**(1): 247-251.

Peterson, R. A., E. C. Buck, J. Chun, R. C. Daniel, D. L. Herting, E. S. Ilton, G. J. Lumetta and S. B. Clark (2018). "Review of the scientific understanding of radioactive waste at the US DOE Hanford Site." Environmental Science & Technology **52**(2): 381-396.

Schröder, D. (2012). "Applications of electrospray ionization mass spectrometry in mechanistic studies and catalysis research." Accounts of Chemical Research 45(9): 1521-1532.

Westesen, A. M., E. L. Campbell, A. N. Williams, A. M. Carney, T. L. Trang-Le and R. A. Peterson (2022). Reduced Temperature Cesium Removal from AP-101 Using Crystalline Silicotitanate, Pacific Northwest National Lab.(PNNL), Richland, WA (United States).

Pacific Northwest National Laboratory

902 Battelle Boulevard
P.O. Box 999
Richland, WA 99354

1-888-375-PNNL (7665)

www.pnnl.gov